PRELIMINARY MEASUREMENTS OF THE ENERGY IMPACT OF INFILTRATION IN A TEST CELL

DAVID E. CLARIDGE, MONCEF KRARTI[1] and SOUVIK BHATTACHARYYA
Energy Systems Laboratory, Department of Mechanical Engineering,
Texas A&M University, College Station.

ABSTRACT

All existing computer models for calculating energy consumption of buildings assume that infiltration increases the heating and cooling load on a building by an amount equal to the mass flow rate of the infiltration times the enthalpy difference between the inside and outside air - with the latent portion of the enthalpy difference sometimes neglected. Recent theoretical and empirical evidence suggests that this approach sometimes, and perhaps often, overstates the energy cost of infiltration. Calorimetric measurements have been conducted on a small test cell with measured amounts of infiltration introduced under conditions: a) where the existing model is expected to give correct results; and b) where the existing model is expected to overstate the energy cost of infiltration significantly. The preliminary data obtained convincingly show that infiltration can lead to a much smaller change in the energy load than is customarily calculated; changes as small as 10 per cent of the calculated value have been measured in a test cell. The data also suggest that the phenomenon occurs in full-sized houses as well.

This leads us to introduce the Infiltration Heat Exchange Effectiveness (IHEE), ϵ, as a measure of the effectiveness of a building in 'recovering' heat otherwise lost (or gained) due to infiltration. Preliminary investigation of possible correlations between the pressure coefficient determined from fan pressurization data and the infiltration heat exchange effectiveness factor, ϵ, suggest that the fan pressurization results may be useful in predicting ϵ for buildings.

INTRODUCTION

Infiltration is one of the major contributors to heating and cooling costs of buildings - especially houses. Knowledge of infiltration and models for predicting the amount of infiltration were very limited until the late 1970s. One of the earliest studies which quantified infiltration in a large number of houses was the work of Caffey [1] who measured air leakage in 50 homes in the Dallas area using an early version of today's fan pressurization technique and quantified the major sites for air leakage in these homes. Based on these measurements, it was concluded that up to 40 percent of the heating and cooling cost of these homes was due to air infiltration.

The contribution of infiltration to heating and cooling requirements varies from house-to-house, but in one comprehensive study of infiltration, Persily [2] ascribed an average of one-third of these requirements to infiltration.

Extensive work has been done on the prediction and measurement of infiltration for building systems, and comprehensive reviews of various methods and models are available [3-5]. But, a very scant amount of research effort has been devoted to the actual energy consumption due to air infiltration. All current computer models for calculating energy consumption of buildings assume that infiltration increases the heating/cooling load on a building by an amount equal to the mass flow rate of the infiltration times the enthalpy difference between the inside and outside air - with the latent portion of the enthalpy difference sometimes neglected. The energy consumption due to infiltration is usually calculated using the simplified equation:

$$Q_{inf} = \dot{m}.c_p.(T_i - T_o) \qquad (1)$$

where:

Q_{inf} = energy consumption due to infiltration (Btu/hr)
$\dot{m}$ = infiltration rate (lb/hr)
c_p = specific heat capacity of air $(Btu/lb - F)$
T_i = indoor temperature (F)
T_o = outdoor temperature (F)

This practice is followed in simple models, such as the Modified Degree-Day method and the Variable-Base Degree-Day method [6], as well as the most complex hourly simulation programs used for research and difficult design problems, including DOE-2.1 [7] and SERIRES [8].

Observations have shown that attic temperatures are often higher than predicted by resistive models of attic insulation. This was first reported by Beyea et.al. [9], who conducted careful experiments on a group of townhouses in Twin Rivers, New Jersey. Claridge et.al. [10] found that attic temperatures in nine of a group of 25 houses examined in the Denver area had less than half the temperature drop expected across attic insulation. These higher attic temperatures are caused by air flow into the attic which bypasses the insulation. The overall loss coefficient calculated for 20 of these houses was 27 to 54 percent higher than values regressed from gas consumption data [11].

Consideration of the combined problem of conduction through insulation and air flow into the attic shows that total heat loss through an attic under these conditions is less than the conduction loss plus the normal exfiltration loss. The attic serves as a heat exchanger and the exfiltrating air, by increasing the attic temperature, reduces the "conductive" loss. Recently, Anderlind [12] has shown that this phenomenon is more general and that energy loss due to infiltration can have a maximum value given by the inside/outside enthalpy difference for the infiltrating/exfiltrating air. He suggests the use of a multiplier R in combination with the coefficient, $(UA)_{inf}$, customarily used. A normalized flow rate parameter is defined and is given by:

$$a = \frac{\dot{m}c_p}{(UA)_w}$$

[1]Current address : Steven Winter Assoc., Norwalk, CT.

Proceedings of the Fifth Symposium on Improving Building Systems in Hot and Humid Climates, Houston, TX, September 12-14, 1988

where $(UA)_w$ is the overall 'UA' value ($Btu/hr-F$) for the walls. For a = 1, the infiltration losses equal conductive losses if $R = 1$. Therefore, the suggested energy lost by infiltration is given by

$$Q_{inf} = R.\dot{m}.c_p.(T_i - T_o) \quad (2)$$

When air leakage enters a wall at one point and travels several feet through the wall before entering the house, it is termed "diffuse" leakage; that which directly enters the building, such as through cracks around a door, is termed "concentrated". Air leakage affects the temperature distribution inside the walls of the building, especially when the air leakage is diffuse.

A new non-dimensional factor, *'Infiltration Heat Exchange Effectiveness'* or IHEE (ϵ), is introduced here. IHEE is the degree of effectiveness of the heat exchange process which occurs when infiltrating/exfiltrating air diffuses through porous insulation. IHEE is simply related to the reduction factor, as defined by Anderlind [16], and is given by:

$$\epsilon = (1 - R) \quad (3)$$

The total heat lost through the walls due to transmission is reduced by diffuse air leakage. This reduction is properly described if the air leakage heat losses are multiplied by a factor, $(1 - \epsilon)$ $(0 \leq \epsilon \leq 1)$ and the transmission losses are calculated in a normal way (i.e. assuming a linear temperature distribution across the walls). Accordingly, the energy lost by infiltration is now given by

$$Q_{inf} = (1 - \epsilon)\dot{m}.c_p.(T_i - T_o) \quad (4)$$

The value of ϵ depends primarily on the relative amounts of diffuse and concentrated air leakage which enter the building envelope.

TEST CELL SET-UP AND EXPERIMENTAL PROCEDURE

EXPERIMENTAL APPARATUS

A set of experiments has been designed to measure the energy impact of controlled amounts of infiltration air in a small test cell. The test cell has been constructed using standard frame construction for the six wall, ceiling and floor surfaces. This construction is:

- 3/8–inch plywood sheathing
- 2x4 studs
- R-11 fiberglass batt insulation between the studs
- 3/8–inch plywood sheathing

The external measurements of the test cell are 56.5–inches wide by 48–inches high by 96–inches long. Each surface was constructed separately, and then, all six were bolted together and caulked; this form of assembly permits replacement or rebuilding of individual surfaces as needed. One of the 56.5–inch by 48–inch end-walls contains a removable 24–inch square window glazed with 3/16–inch plexiglass. This aperture also serves as the door to the test cell between experiments. All joints between the walls and all visible cracks in the wood are tightly caulked to minimize air leakage. The test cell is supported by six large casters to provide portability.

Type T (copper-constantan) thermocouples are used to measure the test cell temperature (including the air inlet and exit temperatures) at nine points as shown in Figure 1. Another sensor is used to measure the temperature outside the test cell. All temperatures are recorded by a programmable data logger.

The pressure difference between the interior and exterior of the test cell is measured using a manometer. The power input for the heater and the fan is determined by measuring the voltage, current and power factor using an AC multimeter. A pressurization test is performed whenever the test cell has been opened to ensure that cell tightness is maintained.

The various holes provided in the test cell for air inlet and outlet are illustrated in Figure 2. Air is introduced through a 0.5–inch hole (hole P) for all the pressurization tests. This hole and a *diffuse* hole (hole B on the exterior) are used as the air inlets in the heating tests to calculate ϵ. The 1.5–inch hole 'E' and another *diffuse* hole (hole A) are used as air outlets. The air flowrate is measured by a rotameter before it enters the test cell.

EXPERIMENTAL PROCEDURE

The test cell is heated by a measured electrical input which powers the heater and the fan which is used to reduce stratification in the test cell. Prior to the experiment, the cell pressurization characteristics were determined by pressurizing the unheated cell and measuring the air flow required to maintain pressure levels ranging from 1-60 Pa. This data was then used to determine the flow constant, k, and the flow exponent, n, of the cell according to the equation

$$Q = k(\Delta P)^n \quad (5)$$

where Q is the air flow rate in cfm and ΔP is the pressure difference in $Pascal$. The value of n is expected to be between 0.5 and 1.0 . For airtight buildings, n is expected to approach 1.0.

The test cell was then heated until steady state conditions were obtained for various inlet flow rates. The temperatures T_i are values measured at different positions within the test cell as indicated in Figure 1. The temperature T_{room} is the temperature measured in the room near the test cell. The average temperature, T_{iav}, within the test cell is taken as the average of all T_i values. The value of the overall UA for the test cell and air flow is calculated as

$$UA = P * 3.413/(1.8 * (T_{iav} - T_{room})) \quad (6)$$

where P is the heating power in Watts, UA is in Btu/hr-F, T_{iav} and T_{room} are in degrees C.

The experimental procedure has been used to test several configurations of the test cell, i.e. different sizes and positions of inlet and outlet holes. The initial experiment was the base case for which infiltration is negligible. In this configuration, the gate valve at exit E is kept closed, and no air is injected into the test cell. For the tests to determine 'ϵ', the following configurations (Figure 2) comprising different air entry and exit arrangements were used :

1. Entry : through hole 'B', exit : none.
2. Entry : through hole 'B', exit : through hole 'A'.
3. Entry : through hole 'B', exit : through holes 'half open E' and 'A'.
4. Entry : through hole 'B', exit : through hole 'E'.

5. Entry : through hole 'B', exit : through holes 'E' and 'A'.
6. Entry : through hole 'P', exit : none.
7. Entry : through hole 'P', exit : through holes 'A' and 'B'.
8. Entry : through hole 'P', exit : through holes 'A', 'B' and 'half open E'.
9. Entry : through hole 'P', exit : through hole 'E'.
10. Entry : through hole 'P', exit : through holes 'A', 'B' and 'E'.

Air flow through holes 'A' or 'B' is termed *diffuse*, and flow through hole 'E' or 'P' is considered *concentrated*. When the exit listed is 'none', there will be a small amount of diffuse leakage through the walls of the test cell. This will also be present in parallel with the other openings used. The explicit diffuse leakage site (hole A or B) consists of two 0.75–inch diameter holes created in the same wall; the first hole is drilled in the exterior plywood, while the second hole is drilled in the interior plywood near the opposite corner of the wall. Thus when air is forced through the exterior hole, it flows inside the wall and enters the test cell through the interior hole. Hole 'E' consists of a 20–inch length of 1.5–inch ID tubing. The 'half open E' refers to a case where a valve is used to reduce the area of 'E' to about half its normal value.

RESULTS

The base case UA represents the steady–state conductive heat loss coefficient of the test cell. Using measured temperatures and heating power in equation (6), for the base case, $UA = 22.06\ Btu/hr - F$. This value is consistent with the calculated value $UA = 21.25\ Btu/hr - F$; corner and edge effects were ignored in the calculated value. Throughout this paper, we assume that in absence of any infiltration, $UA = UA_0 = 22.06\ Btu/hr - F$ and that $\epsilon = 0$. For all other cases, the value of ϵ is calculated from the measured UA value and the injected flow rate $\dot{m}$ as:

$$\epsilon = 1 - \frac{(UA - UA_0)}{(UA)_{inf}} \qquad (7)$$

The difference $(UA - UA_0)$ represents the measured infiltration UA value, while the term $(UA)_{inf} = \dot{m}.c_p$ is the infiltration loss coefficient as usually calculated.

Table 1 shows the results of pressurization measurements for the test cell in various configurations ranging from extremely tight to the leakiest configuration tested. It also shows the leakage coefficient, k, and the air changes per hour for the cell if pressurized to 4 Pa. The units of k provide air flow in cfm when pressure difference is measured in Pa. Each pair of n, k values corresponds to the average resulting from two to six pressurization measurements of the configuration shown. The standard deviation of n is typically 0.03 while that of k is 0.02. The 4 Pa results crudely approximate the rate at which natural infiltration might occur.

Table 1 shows that, when the test cell is sealed and the only leakage occurs through naturally occurring cracks and holes (hole opening = none), n is almost unity, indicating highly diffuse leakage as expected. The air change rate at 4 Pa is less than 0.1 ACH, indicating very tight construction. Addition of the *diffuse* holes (hole opening = B or A,B) increases the leakage appreciably and also lowers the flow exponent to 0.83 and 0.81 respectively, since the flow through these holes is apparently not entirely diffuse. Addition of the large hole (1/2 E, E or combinations of E and A,B) increases the leakage by an order of magnitude and drops the flow exponent to 0.63–0.67, within the range which occurs in typical houses. The air change rate also approximates that of typical houses, although it should be observed that the surface to volume ratio of the test cell is approximately three times that of a typical house, so direct comparisons can be misleading.

INFILTRATION HEAT EXCHANGE EFFECTIVENESS

The Infiltration Heat Exchange Effectiveness (IHEE) is shown as a function of the normalized flow rate a for different flow configurations in Figures 3–4. For the range of flow rates examined, ϵ appears to be an essentially linear function of a within measurement error. Consequently, for purposes of this discussion, we approximate ϵ by

$$\epsilon = \epsilon(0) + m.a \qquad (8)$$

The values $\epsilon(0)$, m and the range of a used to determine $\epsilon(0)$ and m are summarized in Table 2.

We observe that in all cases the slope m is negative and $0 < \epsilon(0) < 1$ as expected. Examination of Figures 3 and 4 also shows that $0 < \epsilon < 1$ for all values of a for which measurements were conducted. This appears to be the most significant result of the preliminary measurements. The values of IHEE are greater than zero for every case measured, indicating that the standard procedure for calculating infiltration loads systematically overestimates infiltration loads. Furthermore, the measurements verify that nearly perfect infiltration heat exchange effectiveness can be measured in frame construction (Figure 3a).

The data shown in Table 2 and Figures 3 and 4 can also be used to construct other hypotheses which should be investigated. These include the following :

1. For cases where the flow into or out of the test cell is highly diffuse (Figures 3a and 4a), the slope is much larger than for concentrated flow; however, the range of a measured was small for these cases since the cell was very tight and larger values of flow would have required pressures above 60 Pa, the upper limit used.
2. In about half the cases, the slope m is about half the value of $\epsilon(0)$. On physical grounds, we expect that m will be less than ϵ for large values of flow.
3. There may be significant departures from the simple linear model of Equation (8) at very low flows $(a < 0.1)$ as suggested by Figures 3 and 4.

DEPENDENCY OF ϵ ON FLOW EXPONENT

The values of ϵ at $a = 0$, as obtained from the best fit linear regression, were correlated to the average values of n obtained from the pressurization tests. Each pair of ϵ and n corresponds to a particular airflow pattern which is characterized by a configuration identification and hole opening.

Figures 5 and 6 present the results of these correlations for the diffuse and concentrated entry configurations, respectively in the zero flow limit ($a = 0$). Figures 7 and 8 likewise show the pattern of variation of ϵ with n at moderate flow rates ($a = 0.5$). In all four cases, a clear correlation between the two parameters can be seen.

To obtain a greater insight into the correlation between the effectiveness, ϵ and the flow exponent, n, the slope, m, of the ϵ–a correlation is plotted as a function of n in Figures 9 and 10 for concentrated and diffuse entry configurations, respectively. Each pair (m, n) corresponds to a particular airflow pattern characterized by a configuration identification and a particular gate valve opening. As is evident from both figures, a fairly strong linear correlation exists. Both figures show that for small values of n (i.e., a leaky cell), the slope m is small indicating that the factor ϵ remains fairly constant with change in the infiltration rate. The results suggest that the effectiveness ϵ is correlated to the flow exponent, n, and the flow rate, $\dot{m}$.

CONCLUSION

The results presented clearly show that air flow through frame construction can exhibit significant heat exchange, greatly reducing the energy requirements on the test cell due to infiltration. Infiltration heat exchange effectiveness values as large as 0.9 have been measured, which indicate that for very tight construction, it is possible that conventional estimates of the infiltration load based on air exchange estimates, could be in error by as much as a factor of 10. However, for the range of values of the pressurization exponent n typically measured in houses, values of IHEE measured in the test cell were much smaller but still suggest that estimates of infiltration load based on air exchange rates are likely to exhibit systematic errors of 10–20 percent.

Examination of the dependence of IHEE on flow rate and flow exponent suggests that for typical flow rates, the flow exponent will provide useful predictive information regarding the size of IHEE and hence, can be incorporated into a procedure for modifying infiltration load calculation procedures for houses.

ACKNOWLEDGMENT

Support for this work was provided by the Center for Energy and Mineral Resources, Texas A&M University, College Station, Texas.

REFERENCES

1. Caffey, G.E., "Residential Air Infiltration," *ASHRAE Trans.*, vol. 85, part I, 1979.

2. Persily, A., "Understanding Air Infiltration in Homes," Report PU/CEES #129, Princeton University Center for Energy and Environmental Studies, February, 1982, 335 pp.

3. Etheridge, D.W., "Modeling of Air Infiltration in Single- and Multi-cell Buildings," *Energy and Buildings*, vol. 10, 1988, pp. 185-192.

4. Feustel, H.E. and Kendon, V.M., "Infiltration Models for Multicellular Structures - A Literature Review," *Energy and Buildings*, vol. 8, 1988, pp. 123-136.

5. Liddament, M. and Allen, C., "The Validation and Comparison of Mathematical Models of Air Infiltration," Technical Note AIC 11, *Air Infiltration Centre*, England, 1983.

6. "ASHRAE Handbook: 1985 Fundamentals," *American Society of Heating, Refrigerating and Air-Conditioning Engineers*, Atlanta, GA, 1985, Chap. 28.

7. "DOE-2 Reference Manual," *Los Alamos Scientific Laboratory*," Los Alamos, NM, 1980.

8. "SERI-RES : Solar Energy Research Institute Residential Energy Simulator," version 1.0, *Solar Energy Research Institute*, Golden, CO, 1982.

9. Beyea, J., Dutt, G. and Wotecki, T., "Critical Significance of Attics and Basements in the Energy Balance of Twin Rivers Townhouses," *Energy and Buildings*, vol. 1, 1977, pp. 261.

10. Claridge, David E., Jeon, H. and Bida, M., "Performance Analysis of the Colorado 50/50 Retrofit Program," vol. I, Submitted to the Solar Energy Research Institute by the Univ. of Colorado, Dept. of Civil, Env. & Arch. Engineering, February, 1984, 82 pp.

11. Claridge, David E., Jeon, H. and Bida, M., "A Comparison of Traditional Degree-Day and Variable-Base Degree-Day Predictions with Measured Consumption of 20 Houses in the Denver Area," *ASHRAE Trans.*, vol. 91, part 2, 1985.

12. Anderlind, G., "Energy Consumption Due to Air Infiltration," in *Proceedings of the 3rd ASHRAE/DOE/BTECC Conference on Thermal Performance of the Exterior Envelopes of Buildings*, Florida, 1985.

Exit Hole Opening	n (average)	k (average)	ACPH (4 PA)
None	0.9787	0.051	0.093
B	0.8269	0.105	0.154
A and B	0.8095	0.150	0.216
E	0.6685	1.298	1.537
B and E	0.6712	1.289	1.532
A, B and 1/2 E	0.6705	1.000	1.188
A, B and E	0.637	1.560	1.766

TABLE 1. Pressurization Test Results (Air Entry Through Hole P)

Inlet	Outlet	$\epsilon(0)$	m	Range of a Measured
B	None	0.97	-1.99	0.04 – 0.12
B	A	0.66	-0.51	0.08 – 0.26
B	1/2 E, & A	0.46	-0.25	0.1 – 0.8
B	E	0.37	-0.19	0.1 – 0.8
B	E & A	0.39	-0.37	0.1 – 0.5
P	None	0.79	-1.94	0.04 – 0.14
P	A & B	0.58	-0.28	0.04 – 0.25
P	1/2 E, A & B	0.24	-0.12	0.15 – 0.75
P	E	0.25	-0.14	0.1 – 0.8
P	A, B & E	0.15	-0.08	0.04 – 0.85

TABLE 2. Linearized Dependence of ϵ on a for Different Flow Configuration

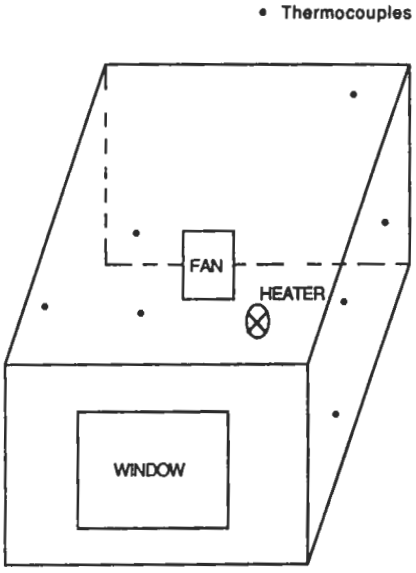

Figure 1. Experimental set-up showing thermocouple locations

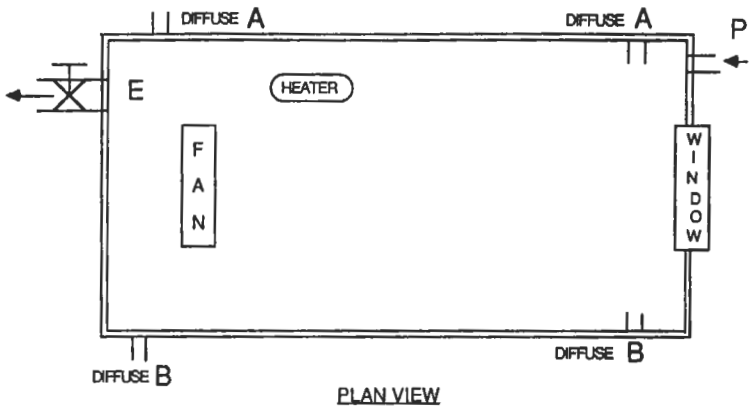

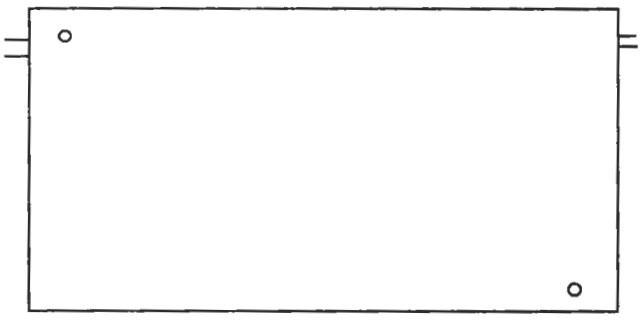

PROFILE VIEW

FIGURE 2. Experimental set-up showing different holes

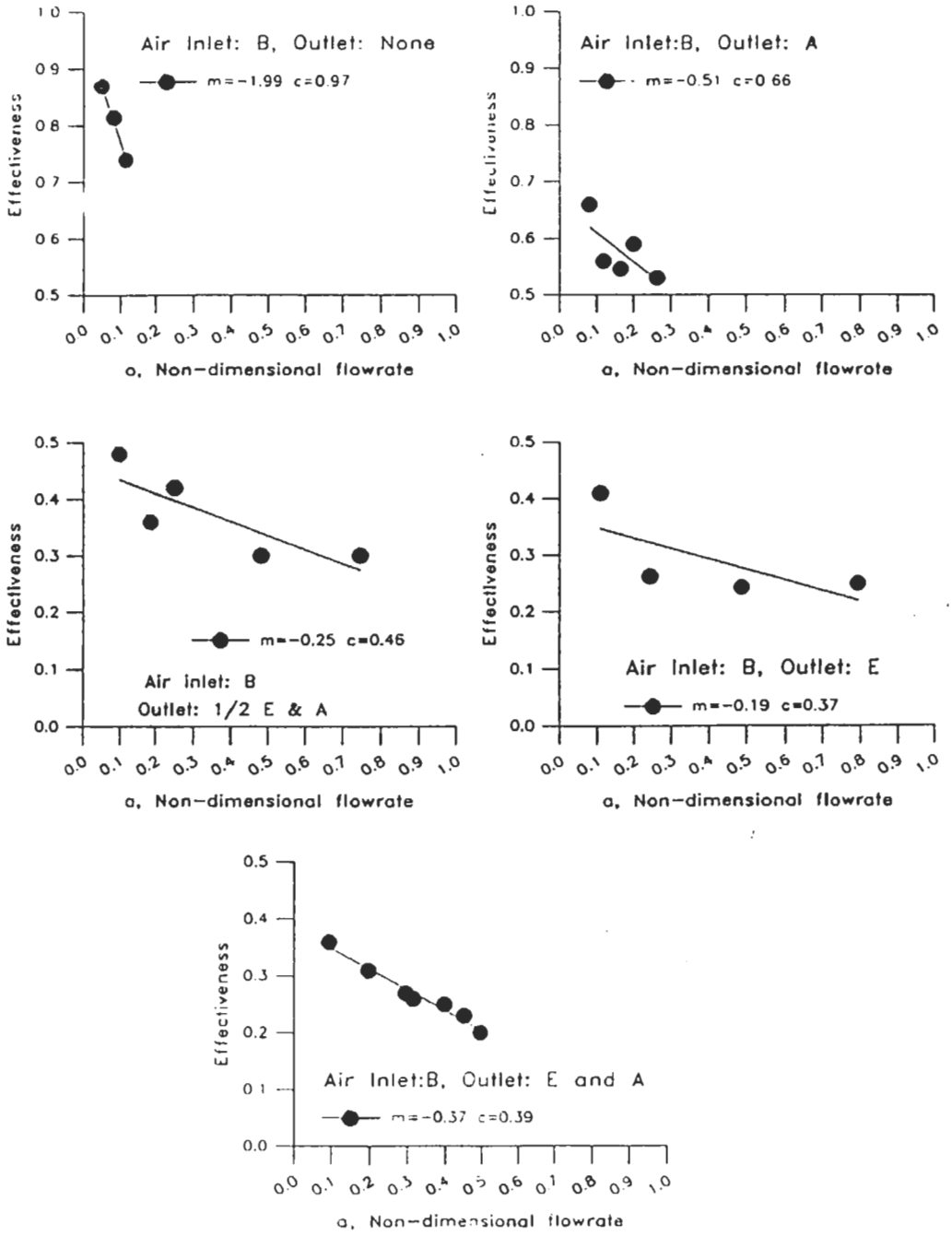

Figure 3. Effectiveness ε vs. non-dimensional flow rate a for `diffuse' inlet and various outlets

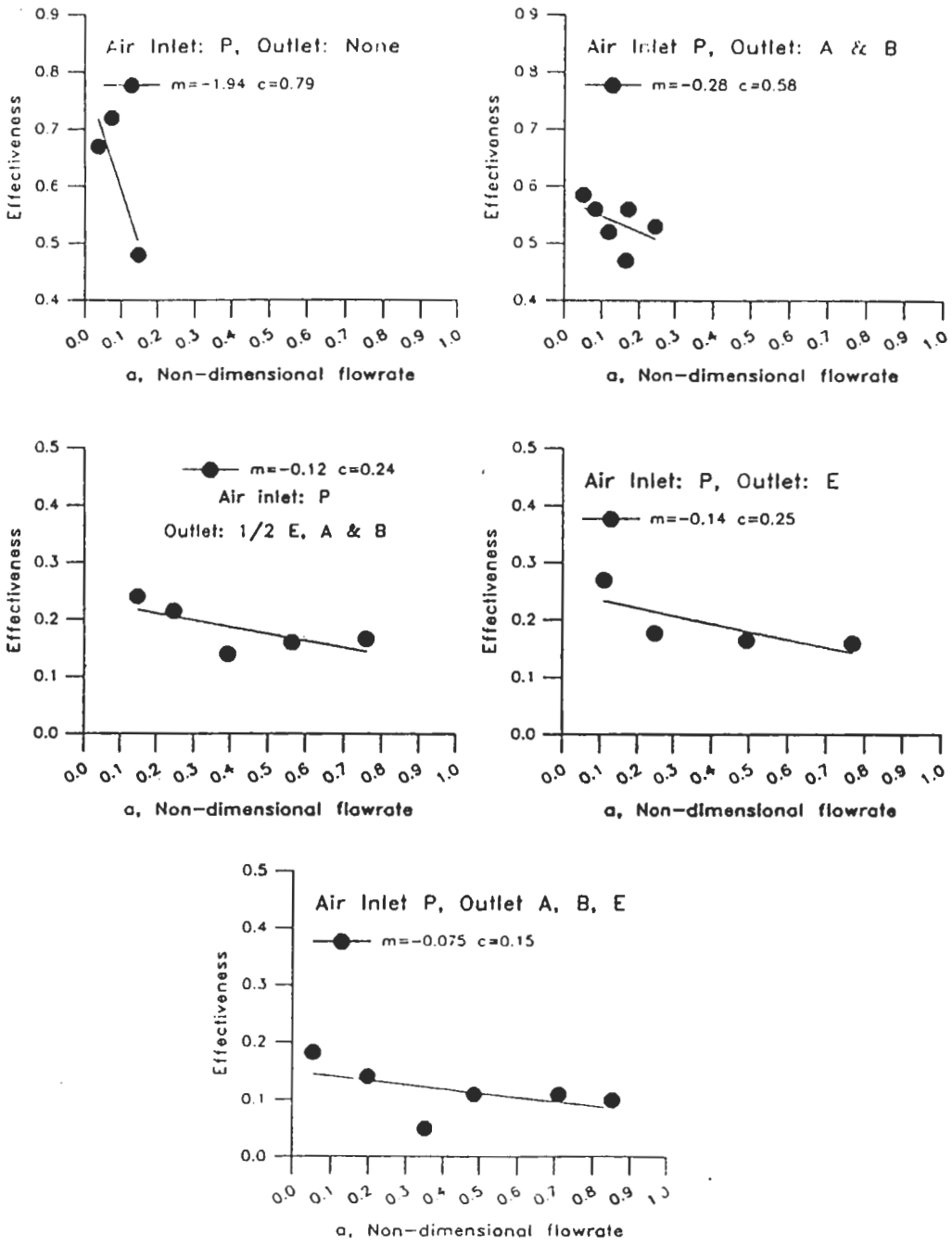

Figure 4. Effectiveness ε vs. non-dimensional flow rate a for `concentrated' inlet and various outlets

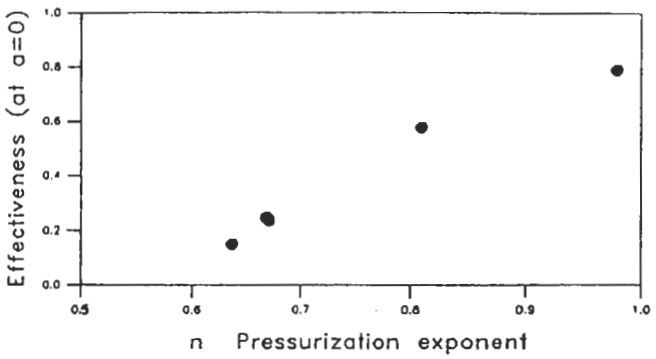

Figure 5. Effectiveness (at a=0) vs. pressurization exponent n for `concentrated' air inlet

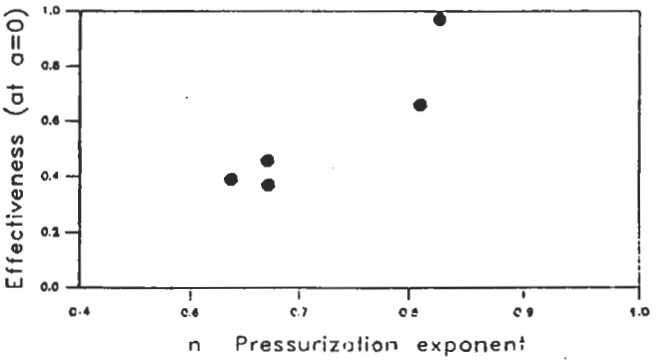

Figure 6. Effectiveness (at a=0) vs. pressurization exponent n for 'diffuse' air inlet

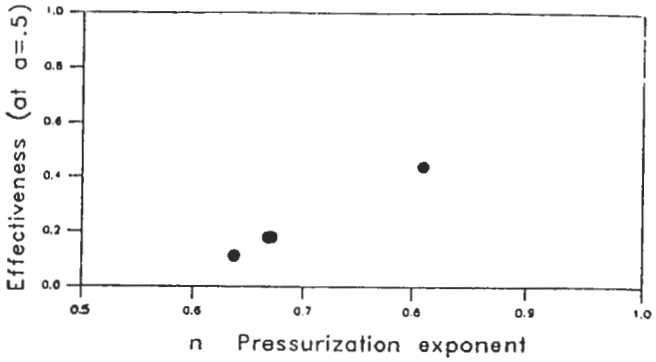

Figure 7. Effectiveness (at a=0.5) vs. pressurization exponent n for 'concentrated' air inlet

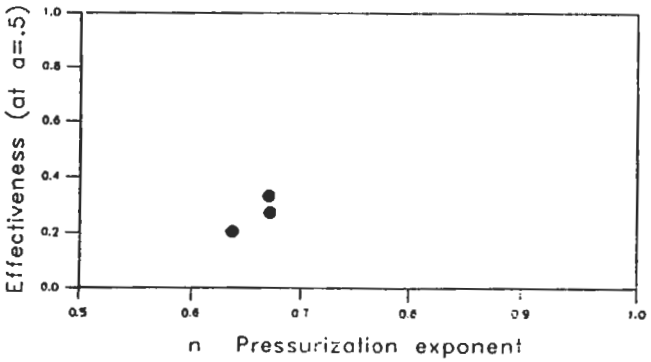

Figure 8. Effectiveness (at α=0.5) vs. pressurization exponent n for 'diffuse' air inlet

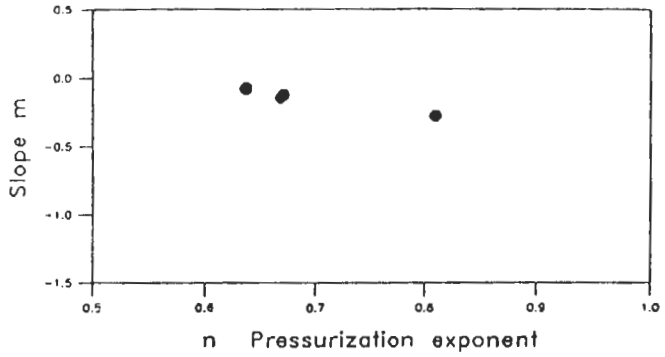

Figure 9. Slope m, of ε-α plot, vs. pressurization exponent n for 'concentrated' air inlet

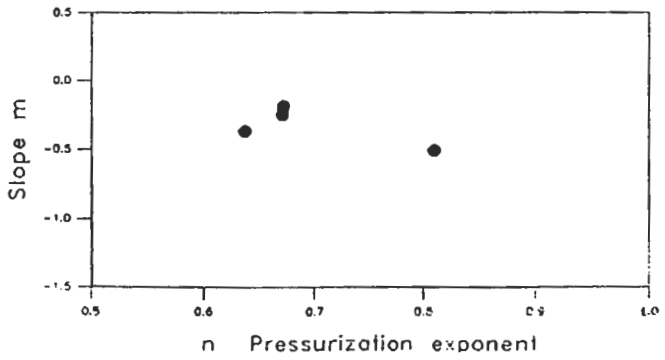

Figure 10. Slope m, of ε-α plot, vs. pressurization exponent n for 'diffuse' air inlet